Inorganic Chemistry

pubs.acs.org/IC

Article

Probing Edge/Support Electronic Cooperativity in Single Edge Fe/Co_6Se_8 Clusters

Benjamin S. Mitchell, Andrei Chirila, Kevin J. Anderton, Werner Kaminsky, and Alexandra Velian*

Cite This: *Inorg. Chem.* 2023, 62, 10497−10503

Read Online

ACCESS | Metrics & More | Article Recommendations | Supporting Information

ABSTRACT: This study provides insights into the electronic structure of an atomically precise Fe/Co_6Se_8 cluster and the extent of redox cooperativity between the Fe active site and the noninnocent Co_6Se_8 support. Chemical oxidation studies enable the isolation of two types of oxidized Fe/Co_6Se_8 clusters, in which the nature of the counterion (I^- or OTf^-) significantly impacts the structural interactions between Fe and the Co_6Se_8 unit. Experimental characterization by single crystal X-ray diffraction, ^{57}Fe Mössbauer spectroscopy, and $^{31}P\{^1H\}$ NMR spectroscopy is complemented by computational analysis. In aggregate, the study reveals that upon oxidation, the charge is shared between the Fe edge site and the Co_6Se_8 core.

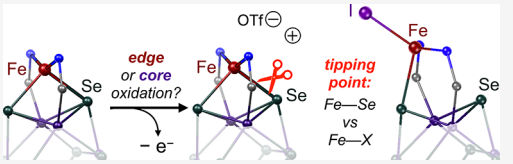

INTRODUCTION

Multimetallic cooperativity holds the promise of imbuing base metals with the ability to achieve desirable multielectron transformations that are uncharacteristic of a single metal.[1] The power of multi-site cooperativity is illustrated by nature's reliance on base metal clusters to carry out some of the most complex and energetically difficult processes, such as cleaving dinitrogen during ammonia biosynthesis.[2,3] Although the mode of operation and electronic structure of the FeMo cofactor are still topics of debate,[4−6] this polymetallic cluster provides the active site for substrate binding and reduction and mediates the transfer of the electrons required for nitrogen fixation.[3,7−9]

Molecular clusters have synthetic tunability to systematically probe and ultimately control how multiple metals interact to achieve complex redox transformations.[10−16] Toward this goal, chemical oxidation studies provide valuable insights and can reveal how the metal identity,[11] ligand binding[17,18] or the ligand framework impact charge distribution within a multimetallic platform.[19−22] For example, inner-sphere oxidation of an all-ferrous Fe_3 cluster was shown to result in anion coordination at one Fe center and localization of the generated charge on the two distal sites.[17] On the contrary, outer-sphere oxidation of a Cu_4S cluster results in complete charge delocalization between the four Cu centers.[18] The Fe_3 and Cu_4S clusters illustrate instances of distinct regimes for multisite electronic interactions in structurally unrelated platforms. By anchoring base metals on the surface of a redox-noninnocent cluster (Co_6Se_8), our group introduced a modular platform that enables access to a range of redox regimes within the same framework.[23−25] Recently, we have shown that the identity of the edge metal M in the single edge clusters $MCo_6Se_8(PEt_3)_4L'_2$ (**1**-M, M = Cr, Mn, Fe, Co, Cu, Zn; L' = $PPh_2N^{(-)}Tol$; Tol = 4-Tolyl, Ph = phenyl, Et = ethyl; Figure 1a) determines the extent to which the active site and the support interact electronically (Figure 1b) and have begun elucidating the consequences of the ensuing cooperativity in catalysis.[25,26]

In this study, we investigate the chemical oxidation of the single-edge cluster **1**-Fe to explicate the extent of edge/support electronic interactions in localizing the resulting charge.[27] ^{57}Fe Mössbauer spectroscopy reveals that the Fe site undergoes oxidation, single crystal X-ray diffraction studies, and $^{31}P\{^1H\}$ NMR spectroscopic analyses, and DFT calculations suggest that the Co_6Se_8 core shares the burden of the charge.

CHEMICAL OXIDATION

Electrochemical measurements have previously revealed that the single edge cluster **1**-Fe, formally $Fe^{2+}/[Co_6Se_8]^0$, can be oxidized reversibly multiple times.[25] Here, the chemical monooxidation of **1**-Fe is accomplished using a series of inner and outer sphere oxidants of appropriate oxidative strength,[28] such as iodine, silver triflate (AgOTf), and ferrocenium hexafluorophosphate ([Fc][PF_6]; Scheme 1). The resulting monooxidized clusters are therefore obtained either as salts [**1**-Fe][X] (X = OTf, PF_6), with the counterion dissociated from Fe as in [**1**-Fe][OTf] or [**1**-Fe][PF_6], or as neutral species with the anion directly bound to the edge site, as in **1**-FeI. From a synthetic standpoint, [Fc][PF_6] is a more convenient reagent, as it enables the isolation of [**1**-Fe][PF_6] as an analytically pure compound (85% yield). While [**1**-Fe][OTf] is not isolated pure, it is characterized in the solid state (Figure 2). The similar spectroscopic signatures of the [**1**-Fe][PF_6] and [**1**-

Received: May 21, 2023
Published: June 15, 2023

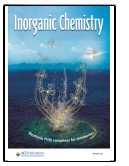

https://doi.org/10.1021/acs.inorgchem.3c01661
Inorg. Chem. 2023, 62, 10497−10503

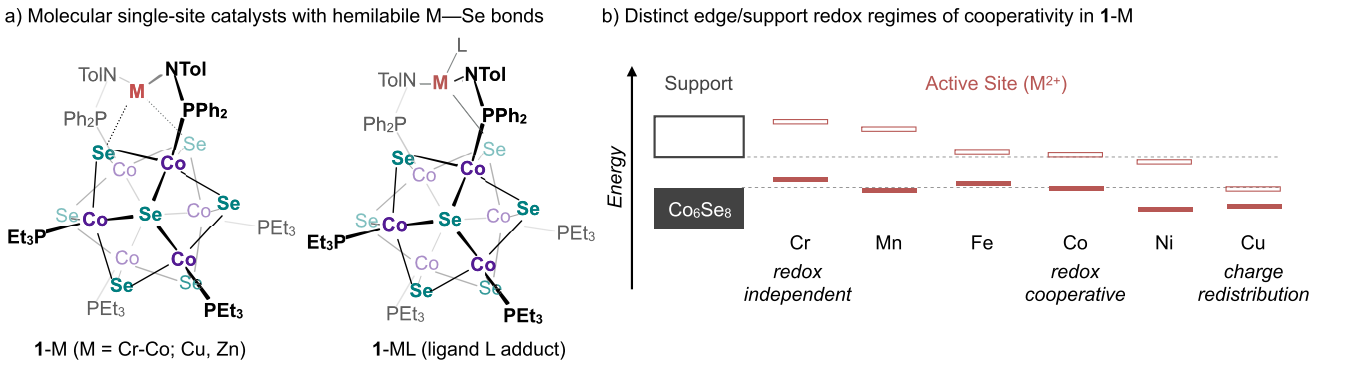

Figure 1. (a) Single edge clusters $MCo_6Se_8(PEt_3)_4L'_2$ (**1**-M; κ^4-M) and monoadduct **1**-ML (κ^3-M). (b) Distinct redox regimes of electronic cooperativity as a result of the energetic and spatial overlap between the edge/support frontier orbitals. Energies approximated from DFT calculations.[25]

Scheme 1. Chemical oxidation of 1-Fe, 1-H_2, and 1-Zn

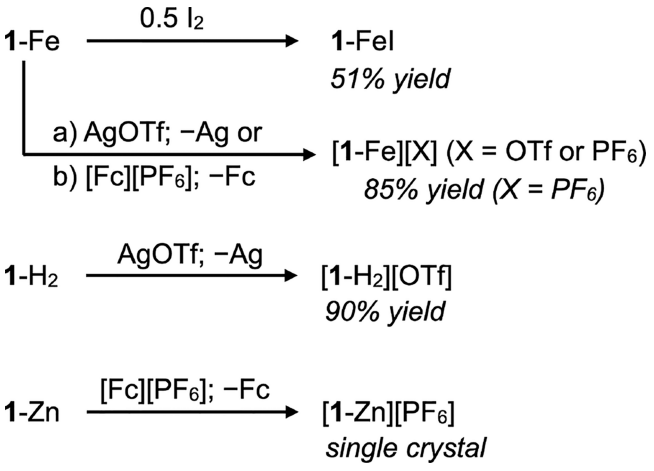

Fe][OTf] salts suggests that in the solid state, the latter is also representative of the former, and the two compounds are considered interchangeable in this text.

The solubility properties of the oxidized clusters align with the extent of anion association at Fe. In contrast to **1**-FeI, the hexafluorophosphate salt [**1**-Fe][PF_6] is insoluble in nonpolar solvents (i.e., toluene, benzene). Interestingly, [**1**-Fe][OTf] readily dissolves in benzene, suggesting that a closer association of the ions occurs in this solvent. ^{19}F NMR spectroscopy indicates that while the triflate ion remains completely dissociated from the Fe edge in polar solvents (δ = −78 ppm in acetonitrile-d_3), it is weakly associated in nonpolar ones (δ = −60 ppm in benzene-d_6).[29]

To compare the structural and electronic changes incurred in the Fe/Co_6Se_8 cluster upon oxidation, **1**-Zn and **1**-H_2 which feature either a redox inactive edge metal (Zn) or no edge metal at all are also oxidized and analyzed. The cluster ligand salt [**1**-H_2][OTf] is produced in good yield (90%) upon treatment with AgOTf. X-ray quality crystals of [**1**-Zn][PF_6] are grown from a crude reaction mixture between **1**-Zn and [Fc][PF_6] (Section S7.3).

STRUCTURAL ANALYSIS

Diffraction quality crystals of [**1**-Fe][OTf] and **1**-FeI are obtained from layered solutions of toluene or benzene-d_6 and *n*-pentane stored at −35 °C (Figure 2). Their analysis illustrates the flexible ligand/active site/support interactions and shines light on the structural changes incurred at the Fe edge upon oxidation of **1**-Fe.[25] Table 1 summarizes key interatomic distances of the clusters discussed in this section.

Binding an exogenous ligand at Fe can occur when the incoming ligand has sufficient coordinative strength to outcompete Se. In turn, the nucleophilicity of the Se sites and the Fe−Se bond strength are responsive to redox changes of the Co_6Se_8 core, the ligand framework, or binding activity at neighboring edge sites when they are present.[26,30] The structures of [**1**-Fe][OTf] and **1**-FeI capture a switching point: iodide is sufficiently nucleophilic to break a Fe−Se bond and give rise to a κ^3-Fe edge in **1**-FeI. In contrast, triflate remains an outer sphere counterion as it cannot outcompete Se

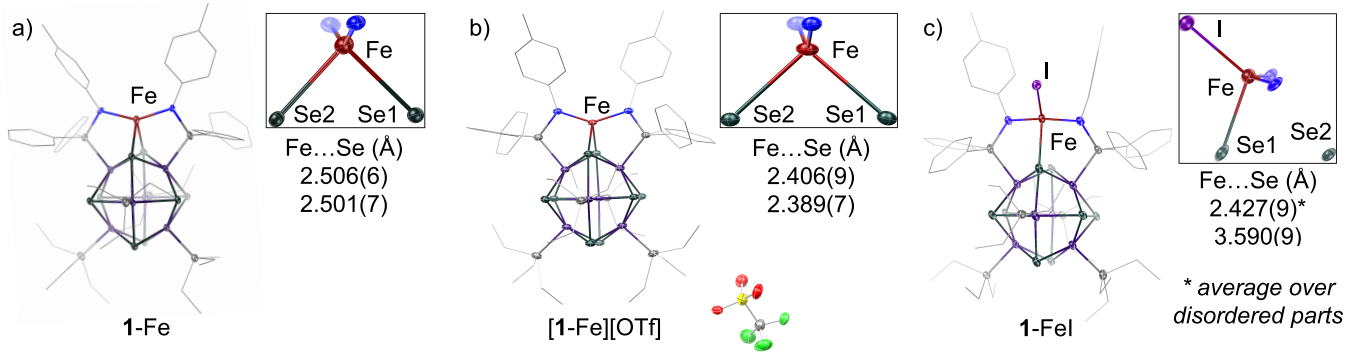

Figure 2. Comparison of bonding metrics at the Fe edge upon mono-oxidation. Single crystal X-ray diffraction of (a) **1**-Fe,[25] (b) [**1**-Fe][OTf], and (c) **1**-FeI. Hydrogen atoms, co-crystallized solvent molecules, and disorder in **1**-FeI are omitted for clarity. Carbon atoms are depicted as wireframe.

https://doi.org/10.1021/acs.inorgchem.3c01661
Inorg. Chem. 2023, 62, 10497−10503

Table 1. Select interatomic distances (Å) for single edge clusters 1-M, and unmetallated clusters $Co_6Se_8L'_6{}^H$ (2-H_6) and [2-H_6][OTf][a]

	intra-Co_6Se_8 (avg, Å)[a]			MCo_2Se_2 edge unit (Å)						
compound	Co−Se	Co···Co	Se···Se	Co−Se	Co···Co	Se···Se	M···Se		M···Co	
1-Fe[b]	2.353(1)	2.940(2)	3.266(2)	2.397(3)	2.890(8)	3.504(8)	2.501(7)	2.506(6)	2.94(1)	2.937(5)
1-FeI	2.345(1)	2.921(1)	3.257(1)	2.354(2)	2.805(3)	3.423(2)	2.61(1)	3.59(1)	3.698(6)	3.65(1)
							2.248(8)	3.46(1)	3.407(7)	3.42(1)
[**1**-Fe][OTf]	2.352(2)	2.916(3)	3.243(3)	2.420(8)	2.85(1)	3.58(1)	2.389(7)	2.406(9)	2.754(6)	2.805(6)
1-Zn[b]	2.350(1)	2.938(1)	3.262(1)	2.382(3)	2.895(6)	3.432(5)	2.537(7)	2.562(7)	3.069(8)	3.087(9)
[**1**-Zn][PF_6]	2.342(2)	2.895(2)	3.257(2)	2.380(3)	2.88(1)	3.44(1)	2.615(8)	2.66(1)	3.104(9)	3.123(9)
2-H_6[b]	2.35(2)	2.944(2)	3.254(2)							
[**2**-H_6][OTf][b]	2.34(1)	2.903(1)	3.260(1)							

[a]Standard error propagation was used to estimate the error for average distances. [b]Previously reported structures.[23,25]

coordination. In [**1**-Fe][OTf], the κ^4-Fe edge site retains the two Fe−Se bonds of the parent complex **1**-Fe, previously characterized in the solid state and depicted in Figure 2a for comparison.[25]

Inspecting the $FeCo_2Se_2$ edge units indicates that anion coordination, as well as oxidation, leads to significant restructuring that propagates through the entire cluster. For example, to accommodate a κ^4-bound Fe edge on the Co_6Se_8 surface, the Co−Se bonds elongate from 2.35 Å in **1**-FeI, to 2.42 Å in [**1**-Fe]$^+$, and the vicinal selenium atoms are pushed apart, increasing the Se···Se interatomic distance from 3.42 to 3.58 Å. Since the average interatomic Co···Se and Se···Se distances of the Co/Se cores remain virtually unchanged, these local distortions are compensated by deformations in the rest of the Co/Se core. Inspecting the edge metrics of [**1**-Fe]$^+$ also reveals that the "appended" Fe center becomes truly incorporated by the Co_6Se_8 cluster. This is reflected in Fe···Co distances of 2.754(6) and 2.805(6) Å that are notably shorter than the average Co···Co distances of the Co_6Se_8 core (2.92 Å).

The edge/support interaction strength (Fe−Se bonds) and the Co···Co distances within the Co_6Se_8 cluster inform on the localization of the charge within the Fe/Co_6Se_8 construct. We hypothesize that if oxidation is localized on the Co_6Se_8 core, the Fe−Se bonds will elongate due to the decreased electron richness of the Se sites. This scenario is illustrated in the mono-oxidized zinc cluster [**1**-Zn][PF_6], where the charge is unambiguously confined on Co_6Se_8, and the two Zn−Se contacts elongate from an average of 2.55 in **1**-Zn to 2.64 Å (Figure S21). Instead, the opposite is observed when oxidizing **1**-Fe in the presence of a weakly coordinating anion: the two Fe−Se bonds contract from an average of 2.50 to 2.40 Å in [**1**-Fe][OTf], suggesting that unlike in the zinc congener, the edge site participates in localizing the charge. As discussed in the next section, Mössbauer spectroscopy corroborates this proposal.

Another empirical structural reporter that adds nuance to this claim is the average interatomic distance between neighboring Co atoms within the Co_6Se_8 core. When oxidation is strictly confined to the Co_6Se_8 core, as is the case in [**1**-Zn][PF_6], **1**-Cu,[25] or [$Co_6Se_8L^H_6$][OTf],[23] the Co···Co average distance consistently contracts from 2.94 to 2.90 avg. Å.[23,31] The Co···Co distance is therefore a reporter on the extent of Co_6Se_8 oxidation between 0/+1 charge. If the charge was completely localized on the Fe center upon monooxidation of **1**-Fe, we would expect an average Co···Co distance of 2.94 Å. Instead, this distance contracts to 2.92 Å in **1**-FeI and [**1**-Fe][OTf], suggesting partial oxidation of the Co_6Se_8 core.

ELECTRONIC INVESTIGATIONS USING MÖSSBAUER SPECTROSCOPY

Two limiting scenarios would localize the charge in [**1**-Fe][X] and **1**-FeI either on the Co_6Se_8 core (Fe^{2+}/[Co_6Se_8]$^{1+}$), or on the iron edge site (Fe^{3+}/[Co_6Se_8]^0). Structural analysis, discussed in the previous section, suggests that the charge is distributed between Fe and Co_6Se_8. Solution phase magnetic measurements using the Evans method[32] confirm, as expected, that [**1**-Fe][OTf] and **1**-FeI have five unpaired electrons each, but do not report on the location of the unpaired electron gained upon oxidation of **1**-Fe. To experimentally probe these possibilities, **1**-Fe, [**1**-Fe][PF_6], and **1**-FeI are analyzed using zero-field ^{57}Fe Mössbauer spectroscopy (Figure 3a). While the neutral **1**-Fe cluster has an isomer shift most consistent with a high spin Fe(II) edge (δ = 0.72 mm/s), the oxidized clusters [**1**-Fe][PF_6] and **1**-FeI have isomer shifts (δ = 0.43, 0.40 mm/s, respectively) typically associated with high spin $Fe^{2.5+}$ or Fe^{3+} centers.[17,33−35] Although the coordination environments of the two κ^4-Fe edges in **1**-Fe and **1**-Fe$^+$ are nearly identical (τ_4 = 0.78 and 0.77, respectively[36]), the shortened Fe−Se bonds, decreased ∠N−Fe−N angle, and electronic changes at Fe give rise to significantly different quadrupole splitting ($|\Delta E_Q|$ = 0.76, 1.01 mm/s, respectively). The quadrupole splitting of **1**-Fe$^+$ is nearly identical to that of **1**-FeI ($|\Delta E_Q|$ = 1.08 mm/s; τ_4 = 0.82), perhaps a reflection of their similar oxidation states and comparable polarizability of Se and I.[37]

In contrast to the tri-Fe clusters $Fe_3Co_6Se_8L_6$' (**Fe_3**) characterized previously by our group,[23] the mono-Fe clusters discussed here incur a significantly stronger response in the ^{57}Fe Mössbauer isomer shifts upon oxidation (Figure 3b). Mössbauer and electrochemical measurements have previously led us to propose that the frontier orbitals of tri-Fe clusters are primarily localized on the Co_6Se_8 core, giving rise to a redox regime wherein the edge sites remain isovalent (Fe^{2+}) upon chemical mono-oxidation or monoreduction.[23] Here, the Mössbauer data indicate that the iron edge undergoes significant oxidation, implying a comparatively lower contribution from the Co_6Se_8 core than in the trimetallated analogues. While limiting scenarios of localizing the charge on the iron or core are attractive in their simplicity, it is also possible, and likely, that *"the distribution of electron density does not occur in 1e$^-$ jumps"*.[38] Therefore, we propose that the charge is distributed between the Fe edge(s) and the cobalt core, to different extents depending on the number of edge

https://doi.org/10.1021/acs.inorgchem.3c01661
Inorg. Chem. 2023, 62, 10497−10503

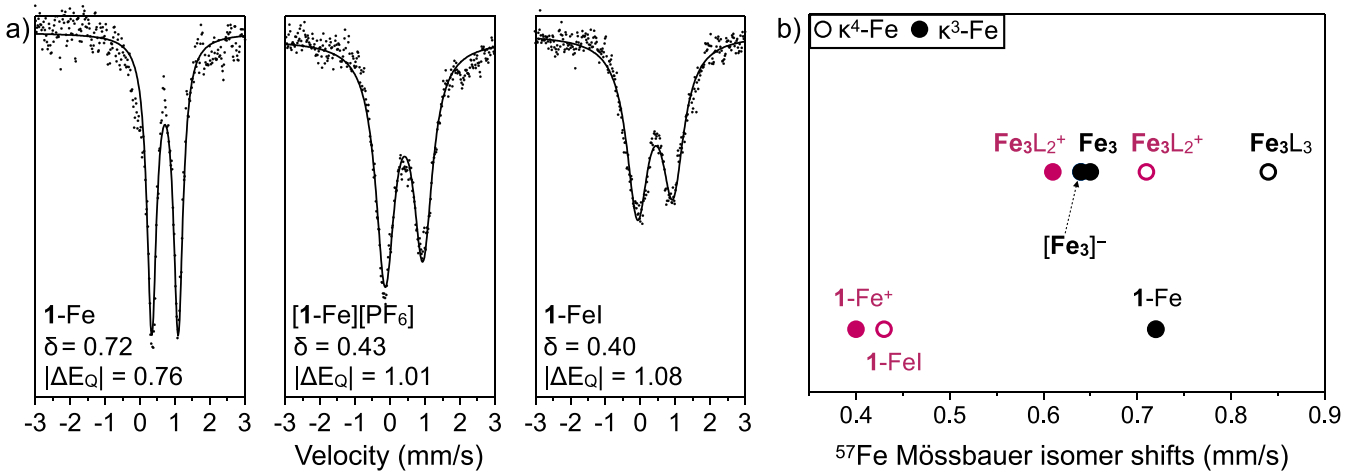

Figure 3. (a) ^{57}Fe Mössbauer spectra of **1**-Fe, **1**-FeI, and [**1**-Fe][PF_6]. (b) Comparison of ^{57}Fe Mössbauer isomer shifts between monoiron (**1**-Fe, **1**-FeI, [**1**-Fe][PF_6]), and triiron (**Fe$_3$**, **Fe$_3$L$_3$**, [**Fe$_3$L$_2$**][PF_6], [TBA][**Fe$_3$**]; L = CN^{t}Bu) clusters redox series. Mono-oxidized clusters are depicted pink and the neutral and monoreduced ones in black.

sites and bound exogenous ligands, placing **1**-Fe and **Fe$_3$** in an intermediate and dynamic edge/support redox regime.[25]

^{31}P{^{1}H} NMR SPECTROSCOPY AND DFT CALCULATIONS INFORM ON EDGE/CORE CHARGE DISTRIBUTION

NMR spectroscopy furnishes detailed insights into the electronic and structural characteristics of the single edge clusters **1**-M.[25] In particular, the ^{31}P{^{1}H} NMR chemical shifts of the phosphines are sensitive reporters for electronic and chemical changes occurring at the edge site (PPh$_2$NTol) or the Co_6Se_8 core (PEt$_3$).

Here, we set out to investigate if the ^{31}P{^{1}H} NMR chemical shifts of **1**-Fe, **1**-FeI, and [**1**-Fe][PF_6] shine light on the relative distribution of charge between the edge and the Co_6Se_8 core and corroborate the findings with electronic structure calculations. Additionally, variable temperature NMR spectroscopy measurements, previously reported[25] for ^{31}P{^{1}H} and appended here for ^{1}H signals, reveal a Curie behavior for **1**-Fe, and inversion recovery experiments enable the complete assignment of the ^{1}H and ^{31}P{^{1}H} NMR signals in **1**-Fe (Figures S15−18).[39,40] Figure 4 compares the ^{31}P{^{1}H} NMR of three pairs of compounds: the κ^4-complexes **1**-Fe/[**1**-Fe][PF_6], the κ^3-complexes **1**-Fe(py)/**1**-FeI, and the parent cluster ligands **1**-H_2/[**1**-H_2][OTf]. The **1**-Fe(py) adduct is presumed to form upon dissolving **1**-Fe in pyridine.[26] The ^{31}P{^{1}H} NMR chemical shifts are also summarized in Table S1.

Oxidation has a large impact on the chemical shift of the PEt_3 groups in the κ^4-Fe complexes **1**-Fe/[**1**-Fe][X], indicating that Co_6Se_8 gains unpaired electron density (Figure 4). Indeed, the PEt_3 groups shift from −113 ppm in **1**-Fe to −632 ppm in the [**1**-Fe]$^+$ cation, whereas the PPh_2NTol groups, already proximal to a paramagnetic center, are minimally affected. The oxidized metalloligand, [**1**-H_2][OTf], which confines the charge exclusively to the Co_6Se_8 core, exhibits a ca. 400 ppm negative shift for both the PEt_3 and the PPh_2NTol groups compared to the neutral cluster **1**-H_2.

The transition from κ^4 to κ^3 coordination at Fe is also associated with diagnostic changes in the ^{31}P{^{1}H} NMR chemical shifts, as seen comparing the [**1**-Fe]$^+$/**1**-FeI and **1**-Fe/**1**-Fe(py) pairs (Figure 4). For example, ligand coordination leads to shifts of ca. 200 ppm to higher frequencies for the PPh$_2$NTol groups in both the neutral and the oxidized clusters. Although distal to the Fe site, PEt_3 are especially sensitive to anion coordination. Two distinct PEt_3 signals are resolved for **1**-FeI clusters, marking their permanent desymmetrization. Their chemical shifts undergo dramatic changes upon anion coordination, from −633 ppm in [**1**-Fe]$^+$ to −355 and −183 ppm in **1**-FeI, the latter ostensibly associated with the distal PEt_3.

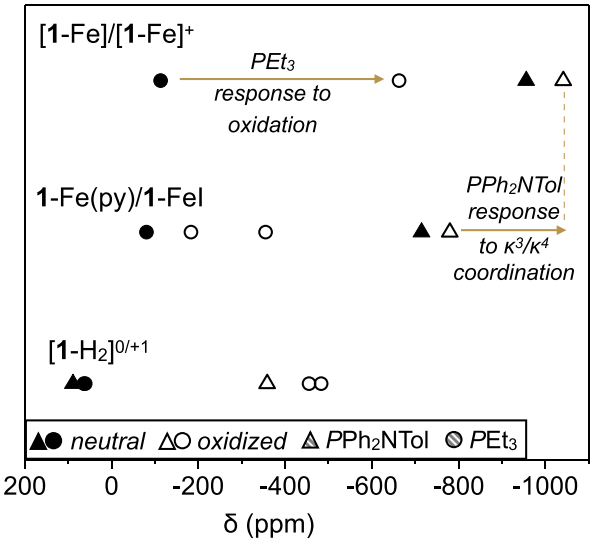

Figure 4. (a) ^{31}P{^{1}H} NMR chemical shifts of amidophosphine PPh_2NTol (triangles) and triethylphosphine PEt_3 (circles) groups in the neutral clusters **1**-H_2, **1**-Fe, and **1**-Fe(py) (filled), and mono-oxidized clusters [**1**-H_2]$^+$, [**1**-Fe]$^+$, and **1**-FeI (hollow).

To probe how the electronic structure of **1**-Fe is impacted by oxidation and anion coordination, we turned to DFT calculations (uB3LYP+/ccpVTZ).[41−44] Figure 5b depicts the Mulliken spin density (α-β) plots for **1**-Fe,[25] **1**-FeI, [**1**-Fe]$^+$, indicating that the spin density on the Co_6Se_8 core more than doubles upon oxidizing the neutral **1**-Fe (0.31) to [**1**-Fe]$^+$ (0.77). These calculations corroborate therefore the proposal

https://doi.org/10.1021/acs.inorgchem.3c01661
Inorg. Chem. 2023, 62, 10497−10503

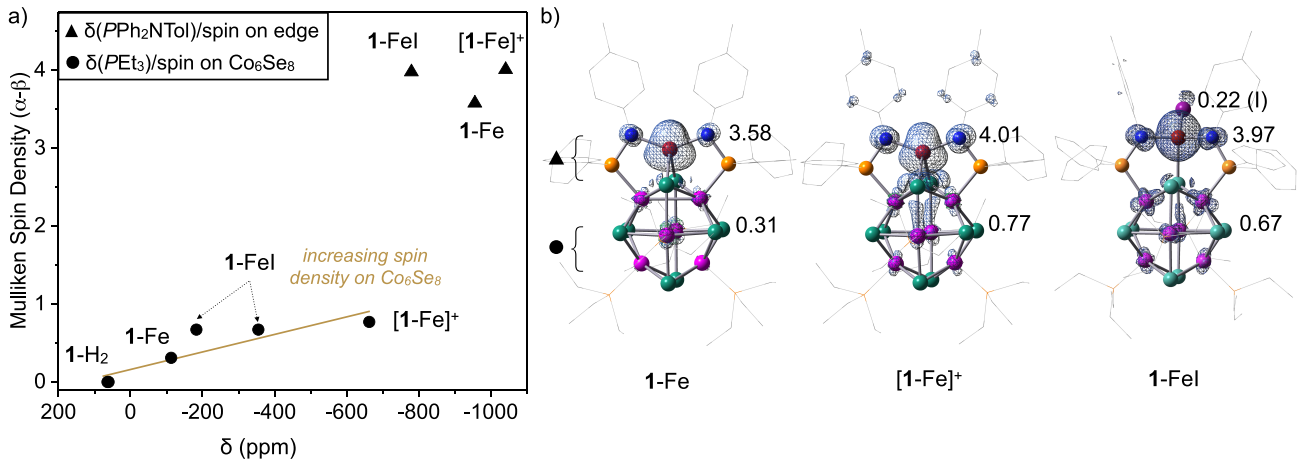

Figure 5. (a) Relationship between the calculated Mulliken spin density (α-β) calculated for the core or edge, and $^{31}P\{^{1}H\}$ NMR chemical shift of PEt_3 and PPh_2NTol. (b) Mulliken spin density (α-β) plots of **1**-Fe, $[\mathbf{1}\text{-Fe}]^+$, and **1**-FeI calculated at the DFT uB3LYP+/cc-pVTZ level of theory.

that the charge is shared between the edge and the Co_6Se_8 support in $[\mathbf{1}\text{-Fe}]^+$.

Since the phosphines report on the electronic structure of the Fe/Co_6Se_8 construct, their $^{31}P\{^{1}H\}$ NMR chemical shifts were plotted against the spin densities calculated for the edge and support (Figure 5a). The $^{31}P\{^{1}H\}$ NMR chemical shifts of the PEt_3 groups on the neutral **1**-H_2 were used as a reference point for a completely diamagnetic cluster. The calculated spin density on the Co_6Se_8 support and experimental $^{31}P\{^{1}H\}$ NMR data for the PEt_3 groups roughly correlate, reaffirming the proposal that upon oxidation of **1**-Fe, the charge is partly localized on the Co_6Se_8 support. At the same time, the relatively small change in the spin density at the edge sites is consistent with minor differences in the chemical shifts of the PPh_2NTol groups in **1**-Fe, **1**-FeI, and $[\mathbf{1}\text{-Fe}]^+$ where the most significant variation occurs as a result of the κ^4 to κ^3 transition at Fe upon anion binding.

CONCLUSIONS

In conclusion, this study reveals atom level insights into the structural and electronic effects of chemical oxidation of **1**-Fe. Outer- and inner-sphere oxidation illustrates the versatility of the cluster construct to accommodate charge and ancillary ligands. The combination of experimental and computational methods highlights an interesting regime of redox delocalization where the charge is shared between the Fe edge and the Co_6Se_8 core.

ASSOCIATED CONTENT

Supporting Information

The Supporting Information is available free of charge at https://pubs.acs.org/doi/10.1021/acs.inorgchem.3c01661.

General experimental considerations, synthetic protocols, and experimental characterization including crystallographic data; NMR studies; DFT optimized geometry coordinates; and computational investigations (PDF)

Accession Codes

CCDC 2225100, 2225102, and 2260994 contain the supplementary crystallographic data for this paper. These data can be obtained free of charge via www.ccdc.cam.ac.uk/data_request/cif, or by emailing data_request@ccdc.cam.ac.uk, or by contacting The Cambridge Crystallographic Data Centre, 12 Union Road, Cambridge CB2 1EZ, UK; fax: +44 1223 336033.

AUTHOR INFORMATION

Corresponding Author

Alexandra Velian − *Department of Chemistry, University of Washington, Seattle, Washington 98195, United States;* orcid.org/0000-0002-6782-7139; Email: avelian@uw.edu

Authors

Benjamin S. Mitchell − *Department of Chemistry, University of Washington, Seattle, Washington 98195, United States;* orcid.org/0000-0001-6585-2237

Andrei Chirila − *Department of Chemistry, University of Washington, Seattle, Washington 98195, United States*

Kevin J. Anderton − *Department of Chemistry and Chemical Biology, Harvard University, Cambridge, Massachusetts 02138, United States*

Werner Kaminsky − *Department of Chemistry, University of Washington, Seattle, Washington 98195, United States;* orcid.org/0000-0002-9100-4909

Complete contact information is available at: https://pubs.acs.org/10.1021/acs.inorgchem.3c01661

Notes

The authors declare no competing financial interest.

ACKNOWLEDGMENTS

Jonathan A. Kephart is acknowledged for thoughtful discussions in preparing the manuscript. This work was supported by the National Science Foundation (NSF) through a Faculty Early Career Development Program Award (1944843) and by the Research Corporation for Science Advancement through a Cottrell Scholars Award. B.S.M. is grateful for support from the NSF Graduate Research Fellowship Program. The authors thank Dylan Rogers for additional assistance with X-ray crystallographic measurements.

https://doi.org/10.1021/acs.inorgchem.3c01661
Inorg. Chem. 2023, 62, 10497−10503

REFERENCES

(1) Cammarota, R. C.; Clouston, L. J.; Lu, C. C. Leveraging Molecular Metal−Support Interactions for H_2 and N_2 Activation. *Coord. Chem. Rev.* **2017**, *334*, 100−111.

(2) Ross, M. O.; Rosenzweig, A. C. A Tale of Two Methane Monooxygenases. *J. Biol. Inorg. Chem.* **2017**, *22*, 307−319.

(3) Hoffman, B. M.; Lukoyanov, D.; Yang, Z.-Y.; Dean, D. R.; Seefeldt, L. C. Mechanism of Nitrogen Fixation by Nitrogenase: The Next Stage. *Chem. Rev.* **2014**, *114*, 4041−4062.

(4) Benediktsson, B.; Bjornsson, R. QM/MM Study of the Nitrogenase MoFe Protein Resting State: Broken-Symmetry States, Protonation States, and QM Region Convergence in the FeMoco Active Site. *Inorg. Chem.* **2017**, *56*, 13417−13429.

(5) Henthorn, J. T.; Arias, R. J.; Koroidov, S.; Kroll, T.; Sokaras, D.; Bergmann, U.; Rees, D. C.; DeBeer, S. Localized Electronic Structure of Nitrogenase FeMoco Revealed by Selenium K-Edge High Resolution X-Ray Absorption Spectroscopy. *J. Am. Chem. Soc.* **2019**, *141*, 13676−13688.

(6) Bjornsson, R.; Neese, F.; DeBeer, S. Revisiting the Mössbauer Isomer Shifts of the FeMoco Cluster of Nitrogenase and the Cofactor Charge. *Inorg. Chem.* **2017**, *56*, 1470−1477.

(7) Arnett, C. H.; Bogacz, I.; Chatterjee, R.; Yano, J.; Oyala, P. H.; Agapie, T. Mixed-Valent Diiron μ-Carbyne, μ-Hydride Complexes: Implications for Nitrogenase. *J. Am. Chem. Soc.* **2020**, *142*, 18795−18813.

(8) Doan, P. E.; Telser, J.; Barney, B. M.; Igarashi, R. Y.; Dean, D. R.; Seefeldt, L. C.; Hoffman, B. M. ^{57}Fe ENDOR Spectroscopy and 'Electron Inventory' Analysis of the Nitrogenase E4 Intermediate Suggest the Metal-Ion Core of FeMo-Cofactor Cycles Through Only One Redox Couple. *J. Am. Chem. Soc.* **2011**, *133*, 17329−17340.

(9) Pickett, C. J.; Vincent, K. A.; Ibrahim, S. K.; Gormal, C. A.; Smith, B. E.; Best, S. P. Electron-Transfer Chemistry of the Iron−Molybdenum Cofactor of Nitrogenase: Delocalized and Localized Reduced States of FeMoco which Allow Binding of Carbon Monoxide to Iron and Molybdenum. *Chem. − Eur. J.* **2003**, *9*, 76−87.

(10) Thomas, C. M. Metal-Metal Multiple Bonds in Early/Late Heterobimetallic Complexes: Applications Toward Small Molecule Activation and Catalysis. *Comments Inorg. Chem.* **2011**, *32*, 14−38.

(11) Eisenhart, R. J.; Clouston, L. J.; Lu, C. C. Configuring Bonds between First-Row Transition Metals. *Acc. Chem. Res.* **2015**, *48*, 2885−2894.

(12) de Ruiter, G.; Carsch, K. M.; Gul, S.; Chatterjee, R.; Thompson, N. B.; Takase, M. K.; Yano, J.; Agapie, T. Accelerated Oxygen Atom Transfer and C−H Bond Oxygenation by Remote Redox Changes in Fe_3Mn-Iodosobenzene Adducts. *Angew. Chem., Int. Ed.* **2017**, *56*, 4772−4776.

(13) Arnett, C. H.; Chalkley, M. J.; Agapie, T. A Thermodynamic Model for Redox-Dependent Binding of Carbon Monoxide at Site-Differentiated, High Spin Iron Clusters. *J. Am. Chem. Soc.* **2018**, *140*, 5569−5578.

(14) Amtawong, J.; Nguyen, A. I.; Tilley, T. D. Mechanistic Aspects of Cobalt−Oxo Cubane Clusters in Oxidation Chemistry. *J. Am. Chem. Soc.* **2022**, *144*, 1475−1492.

(15) Kim, Y.; Sridharan, A.; Suess, D. L. M. The Elusive Mononitrosylated $[Fe_4S_4]$ Cluster in Three Redox States. *Angew. Chem., Int. Ed.* **2022**, *61*, No. e202213032.

(16) Brown, A. C.; Thompson, N. B.; Suess, D. L. M. Evidence for Low-Valent Electronic Configurations in Iron−Sulfur Clusters. *J. Am. Chem. Soc.* **2022**, *144*, 9066−9073.

(17) Eames, E. V.; Betley, T. A. Site-Isolated Redox Reactivity in a Trinuclear Iron Complex. *Inorg. Chem.* **2012**, *51*, 10274−10278.

(18) Johnson, B. J.; Antholine, W. E.; Lindeman, S. V.; Graham, M. J.; Mankad, N. P. A One-Hole Cu_4S Cluster with N_2O Reductase Activity: A Structural and Functional Model for CuZ*. *J. Am. Chem. Soc.* **2016**, *138*, 13107−13110.

(19) Hernández Sánchez, R.; Zheng, S.-L.; Betley, T. A. Ligand Field Strength Mediates Electron Delocalization in Octahedral $[(^{H}L)_2Fe_6(L')_m]^{N+}$ Clusters. *J. Am. Chem. Soc.* **2015**, *137*, 11126−11143.

(20) Arnett, C. H.; Kaiser, J. T.; Agapie, T. Remote Ligand Modifications Tune Electronic Distribution and Reactivity in Site-Differentiated, High-Spin Iron Clusters: Flipping Scaling Relationships. *Inorg. Chem.* **2019**, *58*, 15971−15982.

(21) Hernández Sánchez, R.; Champsaur, A. M.; Choi, B.; Wang, S. G.; Bu, W.; Roy, X.; Chen, Y.-S.; Steigerwald, M. L.; Nuckolls, C.; Paley, D. W. Electron Cartography in Clusters. *Angew. Chem., Int. Ed.* **2018**, *57*, 13815−13820.

(22) Brown, A. C.; Suess, D. L. M. Valence Localization in Alkyne and Alkene Adducts of Synthetic [Fe4S4]+ Clusters. *Inorg. Chem.* **2023**, *62*, 1911−1918.

(23) Kephart, J. A.; Mitchell, B. S.; Chirila, A.; Anderton, K. J.; Rogers, D.; Kaminsky, W.; Velian, A. Atomically Defined Nanopropeller $Fe_3Co_6Se_8(Ph_2PNTol)_6$: Functional Model for the Electronic Metal−Support Interaction Effect and High Catalytic Activity for Carbodiimide Formation. *J. Am. Chem. Soc.* **2019**, *141*, 19605−19610.

(24) Kephart, J. A.; Mitchell, B. S.; Kaminsky, W.; Velian, A. Multi-Active Site Dynamics on a Molecular Cr/Co/Se Cluster Catalyst. *J. Am. Chem. Soc.* **2022**, *144*, 9206−9211.

(25) Mitchell, B. S.; Chirila, A.; Kephart, J. A.; Boggiano, A. C.; Krajewski, S. M.; Rogers, D.; Kaminsky, W.; Velian, A. Metal−Support Interactions in Molecular Single-Site Cluster Catalysts. *J. Am. Chem. Soc.* **2022**, *144*, 18459−18469.

(26) Mitchell, B. S.; Chirila, A.; Zhou, D. Y.; Kephart, J. A.; Velian, A. Metal/Support Interactions Regulate Substrate Binding in Fe/Co/Se Cluster Catalysts. *Inorg. Chem.* **2023**, *62*, 8789−8793. DOI: 10.26434/chemrxiv-2022-f19xz.

(27) Mitchell, B. S.; Chirila, A.; Anderton, K.; Kaminsky, W.; Velian, A. Probing Edge/Support Electronic Cooperativity in Single Edge Fe/Co_6Se_8 Clusters. *ChemRxiv* **2022**, DOI: 10.26434/chemrxiv-2022-4mtw9.

(28) Connelly, N. G.; Geiger, W. E. Chemical Redox Agents for Organometallic Chemistry. *Chem. Rev.* **1996**, *96*, 877−910.

(29) England, J.; Britovsek, G. J. P.; Rabadia, N.; White, A. J. P. Ligand Topology Variations and the Importance of Ligand Field Strength in Non-Heme Iron Catalyzed Oxidations of Alkanes. *Inorg. Chem.* **2007**, *46*, 3752−3767.

(30) Mitchell, B. S.; Krajewski, S. M.; Kephart, J. A.; Rogers, D.; Kaminsky, W.; Velian, A. Redox-Switchable Allosteric Effects in Molecular Clusters. *JACS Au* **2022**, *2*, 92−96.

(31) Choi, B.; Yu, J.; Paley, D. W.; Trinh, M. T.; Paley, M. V.; Karch, J. M.; Crowther, A. C.; Lee, C.-H.; Lalancette, R. A.; Zhu, X.; Kim, P.; Steigerwald, M. L.; Nuckolls, C.; Roy, X. Van Der Waals Solids from Self-Assembled Nanoscale Building Blocks. *Nano Lett.* **2016**, *16*, 1445−1449.

(32) Evans, D. F. 400. The Determination of the Paramagnetic Susceptibility of Substances in Solution by Nuclear Magnetic Resonance. *J. Chem. Soc.* **1959**, 2003−2005.

(33) Fultz, B. Mössbauer Spectrometry. In *Characterization of Materials*; John Wiley & Sons, Ltd, 2012, 1−21.

(34) Pandelia, M.-E.; Lanz, N. D.; Booker, S. J.; Krebs, C. Mössbauer Spectroscopy of Fe/S Proteins. *Biochim. Biophys. Acta* **2015**, *1853*, 1395−1405.

(35) Spreer, L. O.; Li, A.; MacQueen, D. B.; Allan, C. B.; Otvos, J. W.; Calvin, M.; Frankel, R. B.; Papaefthymiou, G. C. Characterization of a Delocalized Mixed-Valence Bis-Macrocyclic Diiron Compound. *Inorg. Chem.* **1994**, *33*, 1753−1755.

(36) Yang, L.; Powell, D. R.; Houser, R. P. Structural Variation in Copper(I) Complexes with Pyridylmethylamide Ligands: Structural Analysis with a New Four-Coordinate Geometry Index, T4. *Dalton Trans.* **2007**, *9*, 955−964.

(37) Rumble, J. *CRC Handbook of Chemistry and Physics*, 103rd ed.; CRC Press/Taylor and Francis: Boca Raton, FL, 2022.

(38) Wolczanski, P. T. Flipping the Oxidation State Formalism: Charge Distribution in Organometallic Complexes As Reported by Carbon Monoxide. *Organometallics* **2017**, *36*, 622−631.

(39) Williams, T. J.; Kershaw, A. D.; Li, V.; Wu, X. An Inversion Recovery NMR Kinetics Experiment. *J. Chem. Educ.* **2011**, *88*, 665−669.
(40) Bernassau, J.-M.; Hyafil, F. Choice of Delay Time Sequence in Spin-Lattice Relaxation Time Measurements by Inversion-Recovery. *J. Magn. Reson. (1969)* **1980**, *40*, 245−258.
(41) Frisch, M. J.; Trucks, G. W.; Schlegel, H. B.; Scuseria, G. E.; Robb, M. A.; Cheeseman, J. R.; Scalmani, G.; Barone, V.; Petersson, G. A.; Nakatsuji, H.; Li, X.; Caricato, M.; Marenich, A. V.; Bloino, J.; Janesko, B. G.; Gomperts, R.; Mennucci, B.; Hratchian, H. P.; Ortiz, J. V.; Izmaylov, A. F.; Sonnenberg, J. L.; Williams; Ding, F.; Lipparini, F.; Egidi, F.; Goings, J.; Peng, B.; Petrone, A.; Henderson, T.; Ranasinghe, D.; Zakrzewski, V. G.; Gao, J.; Rega, N.; Zheng, G.; Liang, W.; Hada, M.; Ehara, M.; Toyota, K.; Fukuda, R.; Hasegawa, J.; Ishida, M.; Nakajima, T.; Honda, Y.; Kitao, O.; Nakai, H.; Vreven, T.; Throssell, K.; Montgomery, Jr., J. A.; Peralta, J. E.; Ogliaro, F.; Bearpark, M. J.; Heyd, J. J.; Brothers, E. N.; Kudin, K. N.; Staroverov, V. N.; Keith, T. A.; Kobayashi, R.; Normand, J.; Raghavachari, K.; Rendell, A. P.; Burant, J. C.; Iyengar, S. S.; Tomasi, J.; Cossi, M.; Millam, J. M.; Klene, M.; Adamo, C.; Cammi, R.; Ochterski, J. W.; Martin, R. L.; Morokuma, K.; Farkas, O.; Foresman, J. B.; Fox, D. J. *Gaussian 16 Rev. A.03*; Gaussian, Inc: Wallingford, CT, 2016.
(42) Becke, A. D. Density-functional Thermochemistry. III. The Role of Exact Exchange. *J. Chem. Phys.* **1993**, *98*, 5648−5652.
(43) Kendall, R. A.; Dunning, T. H., Jr.; Harrison, R. J. Electron Affinities of the First-row Atoms Revisited. Systematic Basis Sets and Wave Functions. *J. Chem. Phys.* **1992**, *96*, 6796−6806.
(44) Stephens, P. J.; Devlin, F. J.; Chabalowski, C. F.; Frisch, M. J. Ab Initio Calculation of Vibrational Absorption and Circular Dichroism Spectra Using Density Functional Force Fields. *J. Phys. Chem.* **1994**, *98*, 11623−11627.

https://doi.org/10.1021/acs.inorgchem.3c01661
Inorg. Chem. 2023, 62, 10497−10503